Published in final edited form as:
Virus Res. 2014 April ; 183: 30–40. doi:10.1016/j.virusres.2014.01.018.

The mammalian orthoreovirus bicistronic M3 mRNA initiates translation using a 5′ end-dependent, scanning mechanism that does not require interaction of 5′-3′ untranslated regions

Vidya Sagar and **Kenneth E. Murray**
Department of biological Sciences, Florida International University, Miami, Florida International University, Miami, Florids-33199

Abstract

Mammalian orthoreovirus mRNAs possess short 5′ UTR, lack 3′ poly(A) tails, and may lack 5′ cap structures at late times post-infection. As such, the mechanisms by which these viral mRNAs recruit ribosomes remain completely unknown. Towards addressing this question, we used bicistronic MRV M3 mRNA to analyze the role of 5′ and 3′ UTRs during MRV protein synthesis. The 5′ UTR was found to be dispensable for translation initiation; however, reducing its length promoted increased downstream initiation. Modifying start site Kozak context altered the ratio of upstream to downstream initiation; whereas, mutations in the 3′ UTR did not. Moreover, an M3 mRNA lacking a 3′ UTR was able to rescue MRV infection to WT levels in an siRNA trans-complementation assay. Together, these data allow us to propose a model in which the MRV M3 mRNA initiates translation using a 5′ end-dependent, scanning mechanism that does not require the viral mRNA 3′ UTR or 5′-3′ UTRs interaction.

Keywords

reovirus; translation initiation; scanning; UTRs interaction

Introduction

Efficient eukaryotic mRNA translation initiation requires the 5′ and 3′ terminus of mRNA to interact and form a circular closed loop. Primarily, this is achieved by the interaction of the 5′ cap binding complex, eukaryotic initiation factor eIF4F, with the 3′ poly (A) tail binding protein, PABP (Hershey et al., 2000). Following mRNA circularization, pre-formed scanning competent 43S pre-initiation complexes (40S ribosomal subunit, eIF3, eIF1, eIF1A, eIF5, and the eIF2-GTP-Met-tRNAi^{Met} ternary complex) are loaded onto the unwound 5′ untranslated region (UTR) (~120 nucleotides long) of the mRNA via an eIF4G-eIF3 interaction. This 43S pre-initiation complex scans the 5′ UTR in a 5′ to 3′ direction

*Correspondence to: Dr. Vidya Sagar, vsaga001@fiu.edu.

until it encounters a start codon (AUG), at which time it forms a 48S initiation complex. Following 48S complex formation, GTP hydrolysis induces eIFs to dissociate from the 40S ribosomes, therein allowing the 60S ribosomal subunit to join and form an elongation competent 80S ribosome (Komarova et al., 2009).

Synthesis of all viral proteins is achieved utilizing host translation factors and ribosomes. As such, many viruses produce 5′ capped, 3′ polyadenylated, monocistronic messages that resemble those produced by the host cell. Many other RNA viruses, however, produce noncanonical mRNAs which frequently lack 5′ cap (m7G(5′)pppG(5′)N cap, where N implies for any nucleotide) structures and/or 3′ poly(A) tails (50–200 residue long poly (A) tail following ~90 nucleotides 3′ UTR). They initiate protein synthesis using alternative mechanisms that necessitate only a subset of host translation factors (Gradi et al., 1998; Balvay et al., 2009; Dutkiewicz et al., 2006; Ilkow et al., 2008; Walsh et al., 2008). Viral mRNAs produced without cap structures may possess highly structured 5′ UTRS that promote direct ribosome loading at internal start sites (Balvay et al., 2009; Niepmann, 2009), or they may be 5′ modified by the covalent linkage of a viral protein (VPg, viral protein genome-linked) (Pettersson et al., 1978; Richards et al., 1981). VPg proteins vary in size, structure, and function, but do, in some cases, act as protein cap substitutes; mediating both mRNA stability and ribosomal recruitment (Goodfellow et al., 2005; Tacken et al., 2004). Viral mRNAs produced without 3′ poly(A) tails have evolved at least three mechanisms to complement the absence of the poly(A) tail. These mechanisms include: 1) utilizing highly structured 3′ terminal RNA elements to mediate stability and/or facilitate ribosomal recruitment (Miller et al., 2007; Treder et al., 2008; Wang et al., 2009), 2) circularizing and stabilizing mRNAs via the specific binding of cellular proteins to 3′ terminal sequences (Polacek et al., 2009), or 3) circularizing and stabilizing mRNAs via the specific binding of viral proteins to 3′ terminal sequences (Groft and Burley, 2002; Vende et al., 2000).

The mammalian orthoreoviruses, like the closely related rotaviruses, produce nonpolyadenylated messages (Schiff et al., 2007); however, unlike rotaviruses, it has been reported that MRV synthesizes uncapped secondary messages (the bulk of [+] ssRNA produced in the MRV infected cell) (Skup and Millward, 1980; Zarbl et al., 1980). It has also been reported that MRV infection alters host translation machinery to favor cap-independent translation (Skup et al., 1981; Sonenberg et al., 1981). Accordingly, during late post-infection MRV-infected cells loss their efficiency to translate capped mRNAs, either cellular or viral. Concomitantly, cell's capability to translate reovirus uncapped mRNA increases. In the same line, ability of eIF4G to interact with eIF4E is decreased during MRV infection; however, the integrity of eIF4G is unchanged (Etchison and Fout, 1985; Mosenkis et al., 1985) suggesting modification in the cap binding complex, eIF4F, to exaggerate the host shut off process (Sonenberg et al., 1981). Together, these observations suggest that MRV mRNAs use a novel mechanism to initiate translation. As such, we hypothesized that MRV mRNAs might: 1) utilize a 5′ UTR sequence to facilitate direct loading of ribosomes at translation (internal initiation), 2) utilize a 3′ terminal structure or sequence to mediate translation initiation, or 3) use a 5′ end-dependent, scanning mechanism to initiate protein synthesis.

In the current study, we investigated the role of 5′ and 3′ UTR sequences during MRV mRNA translation. We engineered mutations into the 5′ and/or 3′ UTRs of the bicistronic M3 gene segment of the type 1 Lang (T1L) strain of MRV. The MRV M3 mRNA encodes two in-frame, carboxy-coterminal proteins, μ-NS and μ-NSC (Fig. 1) (Schiff et al., 2007). We chose to analyze translation of the M3 mRNA for two reasons: 1) the two proteins products (μ-NS and μ-NSC) are easily quantified, and 2) determination of μ-NS/μ-NSC ratios allows direct comparison of WT and mutant RNAs by acting as an internal control for experimental differences in transfection efficiency. Utilizing in-vitro and in-vivo translation assays, we determined that the 5′ UTR is dispensable for MRV M3 translation. While the upstream reading frame continued to be translated even when the 5′ UTR was reduced to a single nucleotide, we found that shortenings of the 5′ UTR promoted increased translation of the downstream reading frame relative to the upstream (leaky scanning). Independent modification of the Kozak context of each MRV M3 start site altered the ratio of upstream to downstream initiation (μ-NS/μ-NSC ratio); further demonstrating that ribosomes associate the 5′ terminus of RMV M3 mRNA and scan to the first or second AUG to initiate translation. Removal of the 3′ UTR did not alter the μ-NS/μ-NSC ratio, and an M3 mRNA lacking the complete 3′ UTR was able to rescue infection to WT levels in an siRNA trans-complementation assay. These data demonstrate that 3′ UTR is also dispensable for translation, and further demonstrate that 5′-3′ UTR interaction is not necessary for efficient translation of the MRV M3 mRNA. Collectively, these data allow us to propose a model in which the mammalian reovirus M3 mRNA initiates translation using 5′ end-dependent, scanning mechanism that does not require UTRs interaction.

Results

The 5′ untranslated region of MRV M3 mRNA is not necessary for translation initiation

Previous investigation have shown that leaky scanning, the process by which a scanning 43S PIC bypasses the first AUG codon encountered and initiates protein synthesis at a downstream site, can be induced by moving the 5′ proximal AUG codon closer to the 5′ terminus (Kozak, 1991). Thus, in an effort to evaluate 43S PIC scanning on the 5′ UTR of the MRV M3 mRNA, we engineered deletions into the 5′ UTR of a previously described M3 construct (pBOS36). We generated three mutant M3 constructs denoted: M3-9, M3-4, and M3-1. T7 polymerase used for synthesizing mRNAs initiate the transcription from first G base at the 3′ end (5′-TAATACGACTCACTATAG-3′). This resulted in addition of an extra “G” base at the 5′ UTR terminus of all transcripts. Thus, synthesized WT M3 mRNA indicated in manuscript possesses a 5′ UTR that is nineteen nucleotides in length. Transcription of M3-9 produced an mRNA possessing a 5′ UTR nine nucleotides in length (nts 9–18 were deleted). Transcription of M3-4 produced an mRNA possessing a 5′ UTR four nucleotides in lengths (nts 4–18 were deleted), and transcription of M3-1 produced an mRNA with a 5′ UTR comprising a single G residue (nts 2–18 were deleted) (Fig. 1). In addition to our mutants, we also reproduce two previously described control M3 mRNA, ΔAUG1 (produces μNS) and ΔAUG2 (produces μNS) (Arnold et al., 2008; Busch et al., 2011; Kobayashi et al., 2006), to serve as gel markers for each protein (Fig 1). To evaluate the effect of each mutation on start site selection, we programmed in-vitro, micrococcal nuclease treated rabbit reticulocyte lysate (RRL) translation reactions with 2 μg of in-vitro

transcribed, capped, WT or mutant mRNA, and translated each mRNA in the presence of [^{35}S]methionine at 30°C for 90 minutes. Labeled proteins were resolved by electrophoresis in SDS 8% polyacrylamide gels. Gels were dried, and separated proteins were detected and quantified via phosphorimaging (fig. 2A). Phosphorimage analysis of the radiolabeled gels allowed us to calculate expression ratios (μNS/μNSC ratio) for each construct, which could then be compared directly to the μNS/μNSC ratios of WT constructs (Fig. 2b). These analyses reveled that reducing the length of the 5′ UTR to nine nucleotides resulted in a modest, but statistically significant increase in downstream initiation (reduced μNS/μNSC ratio). These analyses also revealed that further reductions in the length of the 5′ UTR resulted in greater read through of the upstream (μNS) initiation site (Figs 2A and 2B). While these results were not entirely unexpected, we were surprised to observe that the reduction of the 5′ UTR to four or even one nucleotide did not prevent recognition of the upstream initiation site. More surprising was the observation that the upstream site was preferentially recognized on the M3-4 and M3-1 mRNA (μNS: μNSC>1). When the 5, UTR was reduced to lengths of less than 8 nucleotides we consistently observed the appearance of a third protein product (arrow, Fig. 2A, lanes 3–6). This translation product has been described previously, and is believed to be an in-frame translation product produced when ribosomes scan to the third AUG codon (amino acid position 57) (Schiff et al., 2007). As previously described, the ΔAUG1 mutation abrogated μNS synthesis and promoted increased initiation at both AUG2 and AUG_{57} start sites (Fig. 2A lane 5), whereas the ΔAUG2 mutation produced WT levels of μNS, trace levels of μNS, and increased levels of the AUG_{57} translation product (Fig. 2A, lane 6). The leaky nature of the ΔAUG2 mutation is consistent with previous reports demonstrating that near cognate initiation sites, i.e. UUG, have been shown to function with 5–8% WT efficiency (Takacs et al., 2011).

Because RRL are known to support the efficient translation of some non-canonical transcripts (uncapped or leaderless mRNA) (Wakiyama et al., 1997), we sought to determine what effect the M3-9, M3-4 and the M3-1 mutations would have on μNS/μNS C ratios in cells. To address this, we transfected WT or mutant M3 mRNA into BsrT7 cells. At 24 h p.t., cells were collected and lysed, and clarified lysates were analyzed by immunoblotting to detect μNS and μNSC proteins. Following detection, individual proteins were quantified using ImageQuant 7.0 software. These analyses revealed that reducing the length of the 5′ UTR to nine nucleotides resulted in a modest, but significant reduction of the μNS/μNSC ratio, and as was described for in-vitro RRL reactions, greater reductions in the length of the 5′ UTR (M3-4 and M3-1) further reduced the μNS/μNSC ration (Fig. 2C and 2D). The μNS/μNSC ratios observed in transfected BsrT7 cells, however, were more representative of those described for infected cells (Arnold et al., 2008); Miller et al., 2003). Additionally, significant scanning to AUG_{57} was only observed when the upstream start site (AUG1) was abrogated (Fig. 2C, lanes 2–5). Lastly, these data showed that while μNS continued to be translated from the M3-4 and M3-1 constructs, it was no longer the dominant gene product (μNS/μNSC ratio <1) (Fig. 2D). Together these data, in conjunction with the RRL data, suggest that ribosomes associate with the 5′ terminus of MRV M3 mRNA and scan to an appropriate initiation site. These data also suggest that ribosomes access the μNSC start site by scanning past AUG1 (leaky scanning). The translations of uncapped mRNAs were also verified and it was found that it matches the pattern of capped transcript in large

(Supplementary Figure 1). A similar translation product in capped and uncapped transcripts in M3-1 mRNA suggest a possibility of leaderless mRNA like translation where 80 ribosomal subunit are directly assembled on the 5′ AUG (Andreev et al, 2006). The translation product of uncapped M3-8 mRNA (Fig. S1 lane 3) is little different than its capped counterparts (Fig. 2A lane 2). Nevertheless, translation products due to reduction in 5′ UTR length in both capped and uncapped transcripts follows similar pattern.

Altering the Kozak context of upstream and downstream initiation sites alters the μNS: μNSC ratio

To extend the evidence that 43S PICs scan from the 5′ terminus of the MRV M3 mRNA, we designed mutations that altered the Kozak context of either the upstream or the downstream initiation sites. Because the MRV M3 upstream initiation site resides in a near optimal Kozak context, we introduced mutations predicted to reduce initiation efficiency from this site (fig. 3, Bad_1). The downstream initiation site, however, resides in a suboptimal context; thus, mutations were designed to either improve (Fig. 3, $Good_2$) or impair (Fig. 3, Bad_2) initiation efficiency from this site. In total six constructs were generated, in which either the upstream or downstream site was altered (or abrogated) (Fig. 3). To evaluate the effect of each mutation, we used in-vitro, RRL translation reactions and transfected cell assays. Our in-vitro RRL results showed that weakening the context of the upstream start site promoted increased scanning and initiation from AUG2 (Fig. 4A, Lane2, and Fig. 4B). We also observed increased ribosomal scanning to AUG_{57} when AUG1 and AUG2 were independently weakened and/or abrogated (Bad_1-ΔAUG2 and ΔAUG1-Bad_2 constructs, Fig. 4A lanes 3 and 5, respectively). Consistent with these observations, we also found that maintaining AUG2 in a good context prevented scanning to AUG_{57} (Fig. 4A, lane 7). Interestingly, we found that maintaining AUG1 in a good (WT) context resulted in WT μNS/μNSC ratios only when the downstream start site was also maintained in a WT (fig. 4A, lane 1) or a good context (Fig. 4A, lane 6). When the upstream initiation site was maintained in good context and AUG2 was mutated to reduce initiation efficiency (Bad_2), μNS synthesis was consistently inhibited and only traces levels of AUG2 and AUG_{57} translation products were observed (Fig. 4A, lane 4). Repeated sequencing demonstrated that the WT_1-Bad_2 construct possessed only the desired mutation, and stability assays (not shown) ruled out the possibility that the transcript was rapidly degraded.

Translation of mutant M3 mRNAs in transfected BsrT7 cells produced results largely identical to those produced in-vitro; however, the μNS/μNSC ratios obtained from transfected BsrT7 cells were again found to be lower and more reflective of those observed in infected cells (Fig. 4C, and 4D). We also noted, again, that scanning to AUG_{57} in transfected cells only occurs when ribosomal access to AUG1 is reduced (Fig. 4B lanes 3, 6, and 8). Collectively, these and the preceding data strongly support a model in which ribosomes associate with the MRV M3 5′ terminus and subsequently scan to an appropriate initiation site. Alternatively, it is possible that internal initiation analogues to histone H4 translation may occur where ribosome might be loaded near AUG2 and then scanning back to AUG1 (Martin et al., 2011).

The 3′ UTR does not influence MRV M3 start site selection

Because previous reports have demonstrated that the 3′ UTR of MRV S4 mRNA possesses discrete RNA elements that function as both translational enhancers and suppressors (Mochow-Grundy and Dermody, 2001), we investigated the ability of the MRV M3 mRNA 3′ UTR to influence translation efficiency and start site selection. The MRV M3 3′ UTR is 60 nts in length and comprises two elements: the 3′ terminal pentanucleotide, and a 55 nucleotide intervening sequence (Schiff et al., 2007). The 3′ terminal pentanucleotide (5′…$UCAUC_{oh}$ 3′) is conserved in all ten MRV t1L mRNA, whereas the 55 nucleotide intervening sequence is unique to the MRV M3 mRNA (Fig. 5A) (Schiff et al., 2007). To evaluate the roles of the M3 3′ UTR elements during translation, we generated three mutant constructs, which lacked all or part of the 3′ UTR. M3-Δ3′ lacked the entirety of the 3′ UTR. M3-Δ5nt lacked only the conserved 3′ pentanucleotide, and M3-Δ3′+5nt had the intervening sequence deleted (Fig. 5A). To assess the effect of these mutations on μNS/μNSC synthesis, we used in-vitro RRL and transfected cell translation assays. Results from both assays demonstrated that the MRV M3 3′ UTR is not necessary for translation. In-vitro RRL assays showed that removal of any part of the 3′ UTR had little impact on translation efficiency (Fig. 6A, compare lane 3–5), but did modestly suppressed leaky scanning (increased μNS/μNSC ratios) (Fig. 6B). Translation of M3-4 5′ UTR mutants in transfected BsrT7 cells, however, failed to demonstrate any significant differences in translation efficiency or μNS/μNSC ratios relative to WT constructs (Figs. 6B and d6D). Moreover, μNS:μNSC ratios observe in transfected cells were, once again, reflective of those produce in MRV infected cells.

UTRs interaction of MRV M3 transcripts is not required for efficient translation

Our data demonstrate that the length of the 5′ UTR influences start site selection (shortening the 5′ UTR enhances downstream initiation), and also demonstrate that no RNA sequence or structure residing in the 5′ UTR is necessary for translation of either the μNS of μNSC reading frames. Likewise, translation of M3 mRNA lacking the entirety of the 3′ UTR demonstrates that no sequence or structure residing in the 3′ UTR is necessary for translation. As such, these data further suggest that efficient translation of MRV M3 mRNA does not require elements of the 5′ and 3′ UTRs to directly, or indirectly, interact. To shows, more directly, that 5′-3′ interactions are not necessary for M3 translation, we engineered the, above described, 3′ UTR mutations into our M3-1 construct (Fig. 5B). Transcription of the resulting constructs produced capped, non-polyadenylated, leaderless mRNA that were stable and translationally competent in both in-vitro RRL reactions transfected BsrT7 cells (fig 6A, lanes 7–9; and 6b, lanes 6–8). When μNS/μNSC expression ratios of leaderless, 3′ mutant constructs were calculated, we discovered expression patterns comparable to those produce by constructs possessing only the M3-1 5′ UTR mutation (Figs. 6C and 6D; compare to Figs 2C and 2D). Moreover, when total μNS-μNSC concentrations were normalized to GAPDH, no significant differences in translation were observed (data not shown). Combined, these and the preceding data demonstrate that the 3′ UTR is not necessary for translation of the MRV M3 mRNA, and also show that efficient translation of the MRV M3 mRNA is not dependent upon, nor stimulated by, 5′-3′ mRNA interactions.

The 3′ UTR is not necessary for translation of the MRV M3 mRNA in MRV core transfected cells

Previous investigations of rotavirus translation, more recently, orbivirus translation (both Reoviridae family members) have shown that interactions between the conserved 3′ terminal nucleotides and specific viral proteins greatly stimulate translation. Rotavirus NSP3 interacts with a conserved 3′ terminal tetranucleotide (Piron et al., 1998), whereas orbivirus NS1 has been suggested to interact with elements of a conserved 3′ terminal hexanucleotide sequence (Boyce et al., 2012). Because our entire assay analyzed translation of WT or mutant M3 mRNA independent of the full complement of MRV proteins, we sought to evaluate the effects of MRV proteins on the translation of mutant M3 mRNAs. Because 3′ deletion constructs are replication deficient, we could not utilize reverse genetics to generate recombinant M3 mutant viruses. Instead, we used a previously described siRNA trans-complementation assay (Arnold et al., 2008; Kobayashi et al., 2006). This system uses an siRNA that target WT M3 mRNA (Fig. 7A, M3 si-01) to abrogate the production of μNS and μNSC. In the absence of a functional μNS protein the viral factory (a phase dense viral inclusion, which is the putative site of viral genome replication) does not form, and the viral replication cycle is arrested. The replication cycle can, however, be rescued by transfecting the infected cell with a rescue mRNA possessing wobble base mutations that render it resistant to M3 si-01 induced degradation (Fig. 8A, T1L-WB). To test specific RNA sequences necessary for translation, mutations, can be engineered into the rescue mRNA. As such, we engineered four rescue RNAs: T1L-WB (WT), T1L-WB- Δ5′ (Δ5′), T1L-WB-Δ3′ (Δ3′), and T1L-WB- Δ5′Δ3′ (Δ5′Δ3′). Wt possesses intact MRV M3 5′ and 3′ UTRs, Δ5′ is M3-1 engineered in a T1L-WB background, Δ3′ is T1L-WB lacking the entire 3′ UTR, and Δ5′Δ3′ contains both mutations. To evaluate the translation efficiency of each M3 mRNA rescue construct, we transfected BsrT7 cells with T1L cores, or T1L cores + M3 si-01, or T1L cores + M3 si-01 + rescue RNA. When cells were transfected with T1L cores, we observed robust synthesis of μNS and μNSC (Fig. 7B, lane 1), and we observe a dramatic increase in the concentration of infectious virus particles over a 48 hour time course (Fig. 7C, and Fig. 7D lane 1). When cells were transfected with T1L cores and M3 si-01, we could detect neither μNS not μNSC (Fig. 7B lane 6), and replication of the virus was reduced by greater than 5 $\log_{10}$ (Fig. 7C, and Fig. 7D lane 6); however, when the WT rescue RNA (T1L-WB), was transfected along with T1L cores and M3 si-01, we observed synthesis of μNS and μNSC (Fig. 7B, lane 2) and a 1.5 – 2 $\log_{10}$ rescue of viral replication (Fig. 7C, and Fig. 7D lane 2). These finding are consistent with previously published results obtained using this system (Arnold et al., 2008; Kobayashi et al., 2006). When we attempted to rescue MRV infection with either T1L-WB-Δ5′ or T1L-WB-Δ5′Δ3′ we found – consistent with our RRL and transfected cell assays – increased initiation from the downstream (μNSC) start site (Fig. 7B lanes 3 and 5). We also discovered that Δ5′ and Δ5′Δ3′ mRNAs were unable to rescue MRV infection (Fig. 7C, and Fig. 7D lanes 3 and 5). This result is consistent with two previously published reports that demonstrate that μNSC is neither necessary nor sufficient to support factory formation or viral replication (Arnold et al., 2008; Kobayashi et al., 2006). When the Δ3′ construct was used as a rescue RNA we routinely observed μNS and μNSC protein rescue RNA (Fig. 7B lane 4). Moreover, the T1L-WB-Δ3′ construct was able to rescue viral replication to the same extent as the WT rescue construct (Fig. 7C and Fig. 7D lane 4). These results confirm our previous finding, which

show that virus can be recovered by μNS. These data also demonstrate that the 3′ UTR is not necessary for efficient translation of the M3 mRNA, and confirm that 5′-3′ UTR interactions is not necessary for efficient translation of MRV M3 mRNA.

Discussion

Towards understanding MRV mRNA translation initiation and control, we investigated the role of the untranslated regions of the MRV M3 mRNA. In the course of our investigation, five observations concerning the role of the viral 5′ and 3′ UTRs were noted and are presented here. First: the MRV M3 5′ UTR does not contain any sequences or structures necessary for ribosome recruitment. Second: 43 S PICs scan from the MRV M3 5′ terminus. Third: a leaky scanning mechanism is used to gain access to the downstream μNS initiation site. Fourth: the MRV M3 3′ UTR is dispensable for translation, and fifth: direct or indirect interactions of the 5′ and 3′ UTRS of the MRV M3 mRNA is not necessary for efficient translation.

The MRV M3 mRNA 5′ UTR and scanning ribosomes

Data presented in this manuscript strongly support a model, in which MRV M3 mRNAs load ribosomes using a 5′ end-dependent mechanism with subsequent ribosomal scanning to appropriate start sites. This model derives strong support from two observations. First, shortening of the MRV M3 5′ UTR from 18 nts to a single G residue reduces upstream (μNS) initiation and increases downstream (μNSC) initiation, and second, increasing the length of the 5′ UTR of the MRV M3 mRNA by addition of 13 nucleotides prevents leak scanning and inhibits μNSC expression (Busch et al., 2011). Together these data demonstrate that the length of MRV M3 5′ UTR influences start site selection in a manner that is consistent with ribosomal scanning. Specifically these data argue that reducing the length of the 5′ UTR promotes downstream initiation by limiting the RNA-protein contacts necessary to stall scanning ribosomes at the upstream start site, and/or promoting eIF1 mediated destabilization of 48S complexes assembled on mRNA possessing 5′ UTRs ≤ 8 nts (Pestova and Kolupaeva, 2002). Since cellular concentrations of eIF1 were unaltered in transfected BsrT7 cells, a scanning mechanism would predict that 48S complexes assembled at the μNS initiation sites of M3-9, M3-4, or M3-1 mRNAs would be destabilized by eIF1, whereas complexes that bypassed the upstream start site and instead assembled at the μNSC initiation site would not. Thus, upstream initiation would be reduced and the μNS/μNSC ratio decreased (as observed).

Kozak sequence mutations designed to either improve or impair translation initiation from the μNS or μNSC initiation sites were also analyzed, and it was determined that increased start site read-through correlated with a weakened Kozak context, whereas inhibition of read-through correlated with improved Kozak context. These results further contribute to a model in which ribosomes associate with the 5′ terminus of the M3 mRNA and subsequently scan to the μNS start site (or bypass the μNS site to initiate at the μNSC start site). The repeated failure of WT_1-Bad_2 mRNAs to synthesize any detectable μNS, while generating only trace levels of AUG2 and AUG_{57} translation products, intrigued us because a 5′ end-dependent scanning model of translation initiation predicts that these mRNAs

should synthesize WT levels of μNS with diminished μNSC production. Additionally, these mRNAs were expected to show increased translation initiation from AUG_{57}. While translation of mRNAs possessing this mutation deserve additional investigation, we suspect that the Bad_2 mutation (**GAC**AUGU or **UUU**AUGU) resulted in the creation of either an unstable μNS protein or a slippery sequence that induced ribosomal frameshifts. UUU sequences are know to cause ribosomal frameshifts in prokaryotic systems (Farabaugh, 1996; Schwartz and Curran, 1997; Urbonavicius et al., 2001), and may function similarly in some eukaryotic systems (Farabaugh, 1996; Urbonavicius et al., 2001). A −1/+2 frameshift at the downstream start site would result in a ~7 kDa protein being synthesized from the upstream start site, whereas a +1/−2 frameshift at the downstream start site would result in a ~10 kDa protein being produced from the upstream start site (neither of which would be retained on the gel systems used in these assays). Both hypotheses are consistent with the observed results, and are additionally consistent with a scanning/leaky scanning mechanism of initiation for μNS and μNSC. Also, given that the downstream start site is in a weakened Kozak context, the appearance of the AUG_{57} translation product (fig. 4A, lane 3) (derived by leaky scanning through AUG2) would also be expected. Notably, a weak initiation from AUG2 in ΔAUG2 construct may be result of an alternate initiation codon inserted during conversion of AUG to UUG, which was realized later during the experiment. Nonetheless, this leaky nature is consistent with our previous report (UUG). Moreover, both hypotheses are supported by the observation that the Bad_2 mutation is functional (and leaky) in the context of the ΔAUG1 mutation, wherein elongating 80S ribosomes would not assemble until they reached a position downstream of the altered sequence (Fig. 4a lane 5; and 4C, lane 6).

MRV M3 3′ untranslated region

While RNA sequences and/or structural elements residing in the MRV M3 3′ UTR are most certainly necessary for polymerase recognition, and [−]RNA synthesis (genome replication), they do not appear to be necessary for efficient translation of M3 mRNA. This finding was unexpected given a previous report, which demonstrates that discrete RNA sequence elements residing in the 3′ UTR of the MRV S4 transcript function as either translational enhancers or repressors (Mochow-Grundy and Dermody, 2001). In addition, other investigators have proposed that the non-polyadenylated mRNAs produced by bunyaviruses (Blakqori et al., 2009; Vera-Otarola et al., 2010), flaviviruses (Dutkiewicz et al., 2006; Holden and Harris, 2004; Markoff, 2003), rotaviruses (Chizhikov and Patton, 2000), numerous members of the tombusviridae (wu and White, 1999) and lueteoviridae (Miller et al., 2007; Treder et al., 2008) use 3′ UTR sequence elements to mediate efficient mRNA translation.

The observation that the M3 Δ3′ rescue mRNA and the WT M3 rescue mRNA produced comparable quantities and stoichiometries of μNS and μNSC proteins; and rescued MRV replication to comparable levels in an siRNA trans-complementation assay, provides compelling support for the argument that MRV M3 3′ UTR is dispensable for translation. Moreover, the fact that these results were generated in core transfected cells, in which WT levels of cellular and viral proteins were present, suggests that M3 protein synthesis is neither enhanced nor dependent upon the interaction of 3′ UTR sequences with the viral or

cellular proteins. These observations can be further interpreted to suggest that direct and/or indirect interaction of MRV m3 5′ and 3′ UTRs is not required for – nor does it stimulate – efficient protein synthesis.

When considered with the data presented in this report, the observation that the majority of [+]ssRNAs produced in an MRV-infected cell are purported to be uncapped suggests that MRV transcripts may use a novel 5′ end-dependent, cap-independent, IRES independent, 3′ independent mechanism to recruit ribosomes and initiate translation. This idea is consistent with data from previous investigations, which showed that assembly of elongation competent 80S ribosomes at cognate start sites on uncapped, non polyadenylated, RNA pol III transcribed mRNAs occurs via a 5′ end dependent mechanism that requires ribosomal scanning (Gunnery and Mathews, 1995; Gunnery et al., 1997). Since uncapped mRNAs have been shown to be inefficient at recruiting ribosomes in the presence of capped mRNAs under normal growth conditions, but highly efficient during times of cellular stress (gunnery et al., 1997), such a model may offer mechanistic insight into the processes that allow MRV mRNA to benefit from the integrated stress response (Smith et al., 2006) and escape stress granules at times when host mRNAs are inhibited (Qin et al., 2001).

In conclusion, we have determined that the open reading frame of the MRV M3 transcript comprises a minimal template for translation. We have shown that the 5′ and 3′ UTRs are not required for translation, but the length of the 5′ UTR does strongly influence start site selection. We have also shown that direct or indirect interaction of the 5′ and 3′ UTRs is not required for, not does it stimulate, M3 translation. Extension of these findings to all ten MRV transcripts may provide additional mechanistic insight into the processes that govern RMV gene expression and host shutoff.

Materials and Methods

Cells and Viruses

L929 mouse fibroblasts (L-cells) were maintained in suspension at 37°C by daily passage (5×10^5 – 1×10^6 cells/ml) in Joklik's modified minimal essential medium (MEM) (Sigma) supplemented to contain 2% fetal bovine serum (FBS)(HyClone), 2% bovie calf serum (BCS)(HyClone), 1% L-glutamine (Mediatech), and 1% penicillin-streptomycin solution (Mediatech). BsrT7 cells were maintained in Dulbecco's modified Eagle's medium (DMEM) (Invitrogen) supplemented to contain 10% FBS. Third passage L-cell lysate stocks of plaque purified MRV type-1 Lang (T1L) virus were used to generate purified virions (Chandran et al., 1999) and core particles (Broering et al., 2000), as previously described. Virions and core particles were stored at 4°C in 1X virion buffer (150 mM NaCl, 10 mM $MgCl_2$, 10 mM Tris-acetate [pH 7.5]).

Plasmid constructs

The construction of pBOS36 has been described elsewhere (Arnold et al., 2008). pBOS36 is a pet21b+ (Novagen) derivative, in which the complete MRV T1L M3 gene has been cloned downstream of a T7 promoter and upstream of an HDV ribozyme. Linearization of pBOS36 with NotI, followed by in-vitro T7 transcription, results in the synthesis of MRV T1L M3

mRNAs possessing authentic 5′ and 3′ termini. Incorporation of cap analog "m7G(5′)ppp(5′)G" using T7 promoter resulted in addition of a "G" nucleotide in 5′ termini and, in turn, WT transcripts is 19 nucleotides long, 1 base longer than the natural 18 base-pair long M3 5′ UTR. Individual MRV M3 mutant constructs were generated by site-directed mutagenesis of pBOS36 using Pful turbo (Stratagene) and specific MRV M3 primers (Table 1). pBOS36 rescue plasmid (T1L-WB, type 1 Lang wobble base) was constructed by site-directed mutagenesis using the forward primer pBOS36 wobble base (F) and the reverse primer pBOS36 wobble base (R) (Table 1). Mutant rescue plasmids were generated by site-directed mutagenesis of T1L-WB using specific primers (M3-1 and/or Δ3′) (Table1). All mutant constructs were screened by restriction endonuclease digestion, and verified by DNA sequencing.

In-vitro transcription reactions

Following sequence verification, all pBOS36 constructs were linearized with NOtI. Purified linear constructs were used to template mRNA synthesis in in-vitro T7 transcription reactions. Synthesis of capped mRNA was accomplished using AmplicCap-Max T7 high Yield Message Maker Kits (Cellscript). Newly synthesized mRNA was precipitated by addition of 1 volume (20μl) 5M ammonium acetate. Pelleted mRNAs were washed once in ice-cold ethanol (70%), dried, and resuspended in 40 μls of diethylpyrocarbonate (DEPC)-treated water. mRNA integrity was evaluated by electrophoresis in MOPS-formaldehyde, 1.5% agarose gels, visualized by UV transillumination.

In vitro RRL translation assays

RRL translation assays were done by programming methionine deficient rabbit reticulocyte lysates (RRL) (Promega) with 2μg, capped, WT or mutant MRV M3 mRNA and [^{35}S]methionine (15.5 μCi/rxn) (775μCi/ml)) (MP Biomedicals). Reactions were incubated at 30°C for 90 minutes. [^{35}S]methionine-labeled proteins were solubilized in 1 volume of 2X Laemmli sample buffer (125 mM Tris pH 6.8, 40% glycerol, 4% SDS, 0.01% β-mercaptoethanol, and bromophenol blue), heated at 100°C for 5 minutes and resolved by electrophoresis in SDS 8% polyacrylamide gels. Gels were dried, and radiolabelled proteins were visualized and quantified using a Storm 825 phophorimager (GE Healthcare), and Imagequant 7.0 software (GE Healthcare).

Transient transfections

60 mm dishes seeded with BsrT7 cells (2.1×10^6 cells/60mm dish) were grown in antibiotic free DMEM supplemented to contain 10% FBS. Cells were allowed to from nearly confluent monolayers (~80% confluent), after which the medium was aspirated and the cells were washed twice with phosphate-buffered saline (PBS) (137 mM NaCl, 3 mM KCl, 8 mM Na_2HPO_4, 1 mM KH_2PO_4). For tissue culture translation assays, cells were transfected with 4 μg of in-vitro transcribed, capped, WT or mutant MRV M3 mRNA using 10 μl lipofectamine 2000 in 500 μls Optimem reduced serum medium (Invitrogen), as per the manufacturer's instructions. Following a 2h incubation, cells were lysed, and clarified lysates were prepared. Proteins in clarified lysates were separated by electrophoresis in SDS 8%-polyacrylamide gels and transferred to nitrocellulose membranes. μNS, μNSC, and

AUG57 proteins were detected by immunoblotting and quantified by densitometry using Imagequant 7.0 software.

Immunoblotting

BsrT7 cells were plated in 60mm dishes and transfected as describe above. Total proteins were collected and analyzed at the indicated time p.t.. Briefly, culture medium was aspirated from infected monolayers and cells were washed twice in phosphate buffered saline, (PBS, [pH 7.5]: 137 mM NaCl, 8 mM Na_2HPO_4, 1.5 mM KH_2PO_4, 2.7 mM KCL). Cells were collected in PBS-EDTA (5mM), and counted on a hemocytometer. Following quantification, cells were pelleted by low speed centrifugation, and disrupted in lysis buffer (10mM Tris [pH 7.0], 150 mM BaCl, 0.1% NaDOC, 1 mM EDTA, 1% NP40, 0.1% SDS, and 1X complete protease inhibitor (Roche)). After 30 min on ice, samples were clarified by centrifugation at 13,000 × g for 30 min at 4°C. Clarified cell lysates, normalized for cell number, were solubilized in protein sample buffer, heated at 100°C for 5 minutes, resolved by electrophoresis on SDS-polyacrylamide gels and transferred to nitrocellulose membranes. Membranes were blocked in TBST (10 mM Tris [pH 8.0], 150 mM NACl, 0.1% Tween 20) supplemented to contain 5% nonfat dry milk. Membranes were washed with TBST and incubated for 1 h with an appropriately diluted cellular or viral primary antibody. The binding of primary antibodies was detected photographically on X-ray film (Phenix) using an HRP-conjugated anti-mouse or anti-rabbit IgG (Cell Signaling Technologies) diluted in TBST and a Supersignal West Pico chemiluminescence kit (Pierce). The following antibody dilutions were used: rabbit anti-μNS polyclonal serum (Broering et al., 2000) was used at a dilution of 1:40,000, rabbit anti-MRV virion polyclonal serum (Broering et al., 2000) was used at a dilution of 1:10,000, and mouse monoclonal anti-GAPDH antibody (65C) (Santa Cruz biotechnology, Inc.) was used at a dilution of 1:5000. Secondary antibodies: goat anti-rabbit IgG HRP-linked, and horse anti-mouse IgG HRP-linked antibodies (Cell Signaling Technologies) were each used at 1:2500.

siRNA trans-complementation assay

siRNA M3 si-01 (Fig. 7A) targets the MRV M3 [+]ssRNA sequence 5′-UACCUUAUCAGCAUGUGAA-3′. M3 si-01 was obtained from Dharmacon-Thermo Scientific, and was resuspended to a final concentration of 20 μM (20 pmoles/μl), and used at a final concentration of 100 nM in agreement with manufacturer's instructions and previously described reports (Arnold et al., 2008).

siRNA trans-complementation assays were conducted as previously described (Arnold et al., 2008). Briefly, near confluent monolayers of BsrT7 cells, in 6-well plates, were transfected with a combination of MRV T1L core particles (1×10^8 particles), M3 si-01, and in vitro transcribed rescue mRNAs (1μg) using 10μl lipofectamine 2000 in 100 μl Optimem reduced serum medium. Based on the observation that infectious yields were routinely reduced by greater than 5 $logs_{10}$, we estimated that M3 si-01 was transfected with greater than 99% efficiency. Zero time point cells were harvested following transfection, whereas the remainder of transfected cells was incubated at 37°C for an additional 24 or 48 hours. At each time point cells were washed, lysed, and prepared for immunoblot analysis (described above) or viral plaque assays. Plaque assays were conducted on confluent monolayers of

L929 mouse fibroblast grown in six-well plates (as previously described) (Murray and Nibert, 2007).

Supplementary Material

Refer to Web version on PubMed Central for supplementary material.

Acknowledgments

VS was supported, in part, by funding from the Florida International University, Minority Opportunities in Biomedical Research Program, RISE, from NIH/NIGMS (R25 GM061347).

References

Andreev DE, Terenin IM, Dunaevsky YE, Dmitriev SE, Shatsky IN. A leaderless mRNA can bind to mammalian 80S ribosomes and direct polypeptide synthesis in the absence of translation initiation factors. Mol Cell Biol. 2006; 26:3164–3169. [PubMed: 16581790]

Arnold MM, Murray KE, Nibert ML. Formation of the factory matrix is an important, though not a sufficient function of nonstructural protein muNS during reovirus infection. Virology. 2008; 375:412–423. [PubMed: 18374384]

Balvay L, Soto Rifo R, Ricci EP, Decimo D, Ohlmann T. Structural and functional diversity of viral IRESes. Biochim Biophys Acta. 2009; 1789:542–57. [PubMed: 19632368]

Blakqori G, van Knippenberg I, Elliott RM. Bunyamwera orthobunyavirus S-segment untranslated regions mediate poly(A) tail-independent translation. J Virol. 2009; 83:3637–3646. [PubMed: 19193790]

Boyce M, Celma CPC, Roy P. Bluetongue virus non-structural protein 1 is a positive regulator of viral protein synthesis. Virology Journal. 2012; 2012:9, 178.

Broering TJ, McCutcheon AM, Centonze VE, Nibert ML. Reovirus nonstructural protein μNS binds to core particles but does not inhibit their transcription and capping activities. J Virol. 2000; 74:5516–5524. [PubMed: 10823857]

Busch LK, Rodríguez-Grille J, Casal JI, Martínez-Costas J, Benavente J. Avian and mammalian reoviruses use different molecular mechanisms to synthesize their microNS isoforms. J Gen Virol. 2011; 11:2566–2574. [PubMed: 21795469]

Chandran K, Walker SB, Chen Y, Contreras CM, Schiff LA, Baker TS, Nibert ML. In vitro recoating of reovirus cores with baculovirus-expressed outer-capsid proteins μ1 and ς3. J Virol. 1999; 73:3941–3950. [PubMed: 10196289]

Chizhikov VJ, Patton T. A four-nucleotide translation enhancer in the 3′-terminal consensus sequence of the nonpolyadenylated mRNAs of rotavirus. RNA. 2000; 6:814–825. [PubMed: 10864041]

Dutkiewicz M, Swiqtkowska A, Ciesiolka J. Structure and function of the non-coding regions of hepatitis C viral RNA. Postepy Biochem. 2006; 52:62–71. [PubMed: 16869303]

Etchison O, Fout S. Human rhinovirus 14 infection of HeLa cells results in the proteolytic cleavage of the p220 cap-binding complex subunit and inactivate globin mRNA translation in vitro. J Virol. 1985; 54:634–638. [PubMed: 2985827]

Farabaugh PJ. Programmed translational frameshifting. Microbiol Rev. 1996; 60:103–134. [PubMed: 8852897]

Goodfellow I, Chaudhry Y, Gioldasi I, Gerondopoulos A, Natoni A, Labrie L, Laliberte JF, Roberts L. Calicivirus translation initiation requires an interaction between VPg and eIF 4 E. EMBO Rep. 2005; 6:968–972. [PubMed: 16142217]

Gradi A, Svitkin YV, Imataka H, Sonenberg N. Proteolysis of human eukaryotic translation initiation factor eIF4GII, but not eIF4GI, coincides with the shutoff of host protein synthesis after poliovirus infection. Proc Natl Acad Sci. 1998; 95:11089–11094. [PubMed: 9736694]

Groft CM, Burley SK. Recognition of eIF4G by rotavirus NSP3 reveals a basis for mRNA circularization. Mol Cell. 2002; 9:1273–1283. [PubMed: 12086624]

Gunnery S, Mathews MB. Functional mRNA can be gener-ated by RNA polymerase III. Mol Cell Biol. 1995; 15:3597–3607. [PubMed: 7791767]

Gunnery S, Mälvali Ü, Mathews MB. Translation of an uncapped mRNA involves scanning. J Biol Chem. 1997; 272:21642–21646. [PubMed: 9261187]

Hershey, JWB.; Merrick, WC. The pathway and mechanisms of initiation of protein synthesis. In: Sonenberg, N.; Hershey, JWB.; Mathews, MB., editors. Translational Control of Gene Expression. 2. Cold Spring Harbor: Cold Spring Harbor Laboratory Press; 2000. p. 33-88.

Holden KL, Harris E. Enhancement of dengue virus translation: role of the 3′ untranslated region and the terminal 3′ stem-loop domain. Virology. 2004; 329:119–133. [PubMed: 15476880]

Ilkow CS, Mancinelli Beatch VMD, Hobman TC. Rubella virus capsid protein interacts with poly(A)-binding protein and inhibits translation. J Virol. 2008; 82:4284–4294. [PubMed: 18305028]

Kobayashi T, Chappell JD, Danthi P, Dermody TS. Gene-specific inhibition of reovirus replication by RNA interference. J Virol. 2006; 80:9053–9063. [PubMed: 16940517]

Komarova V, Haenni A-L, Ramírez BC. Viruses vs Host cell translation: Love and Hate stories. Advances in virus research. 2009; 73:99–170. [PubMed: 19695382]

Kozak M. A short leader sequence impairs the fidelity of initiationby eukaryotic ribosomes. Gene Expression. 1991; 1:111–115. [PubMed: 1820208]

Markoff L. 5′- and 3′-noncoding regions in flavivirus RNA. Adv Virus Res. 2003; 59:177–228. [PubMed: 14696330]

Martin F, Barends S, Jaeger S, Schaeffer L, Prongidi-Fix L, Eriani G. Cap-assisted internal initiation of translation of histone H4. Mol Cell. 2011; 41(2):197–209. [PubMed: 21255730]

Miller CL, Broering TJ, Parker JSL, Arnold MM, Nibert ML. Reovirus σNS protein localizes to inclusions through an association requiring the μNS amino terminus. J Virol. 2003; 77:4566–4576. [PubMed: 12663763]

Miller WA, Wang Z, Treder K. The amazing diversity of cap-independent translation elements in the 3′-untranslated regions of plant viral RNAs. Biochem Soc Trans. 2007; 35:1629–1633. [PubMed: 18031280]

Mochow-Grundy M, Dermody TS. The reovirus S4 gene 3′ nontranslated region contains a translational operator sequence. Journal of virology. 2001; 75:6517–6526. [PubMed: 11413319]

Mosenkis J, Danlels-McQueen S, Janovec S, Duncan R, Hershey JWB, Grifo JA, Merrick WC, Thach RE. Shut-off of host translation by encephalomyocarditis virus infection does not involve cleavage of the eucaryotic initiation factor 4F polypeptide that accompanies pollovirus infection. J Virol. 1985; 54:643–645. [PubMed: 2985829]

Murray KE, Nibert ML. Guanidine hydrochloride inhibits mammalian orthoreovirus growth by reversibly blocking the synthesis of double-stranded RNA. J Virol. 2007; 81:4572–4584. [PubMed: 17301147]

Niepmann M. Internal translation initiation of picornaviruses and hepatitis C virus. Biochim Biophys Acta. 2009; 1789:529–541. [PubMed: 19439208]

Pestova TV, Kolupaeva VG. The roles of individual eukaryotic translation initiation factors in ribosomal scanning and initiation codon selection. Genes Dev. 2002; 16:2906–2922. [PubMed: 12435632]

Pettersson RF, Ambros V, Baltimore D. Identification of a protein linked to nascent poliovirus RNA and to the polyuridylic acid of negative-strand RNA. J Virol. 1978; 27:357–365. [PubMed: 211265]

Piron M, Vende P, Cohen J, Poncet D. Rotavirus RNA-binding protein NSP3 interacts with eIF4GI and evicts the poly(A) binding protein from eIF4F. EMBO J. 1998; 17:5811–5821. [PubMed: 9755181]

Polacek C, Friebe P, Harris E. Poly(A)-binding protein binds to the non-polyadenylated 3′ untranslated region of dengue virus and modulates translation efficiency. J Gen Virol. 2009; 90:687–692. [PubMed: 19218215]

Qin Q, Carroll K, Hastings C, Miller CL. Mammalian orthoreovirus escape from host translational shutoff correlates with stress granule disruption and is independent of eIF2alpha phosphorylation and PKR. Journal of virology. 2011; 85:8798–8810. [PubMed: 21715487]

Richards OC, HEY TD, Ehrenfeld E. Two forms of VPg on poliovirus RNAs. Journal of Virology. 1981; 38:863–871. [PubMed: 6264160]

Schiff, LA.; Nibert Max, L.; Tyler Kenneth, L. Orthoreoviruses and Their Replication. In: Knipe, DM.; Howley, PM., editors. Fields' virology. 5. Lippincott: Williams and Wilkins; 2007. p. 1853-1916.

Schwartz R, Curran JF. Analyses of frameshifting at UUU-pyrimidine sites. Nucleic Acids Res. 1997; 25:2005–2011. [PubMed: 9115369]

Skup D, Millward S. Messenger-Rna Capping Enzymes Are Masked In Reovirus Progeny Subviral Particles. Journal of virology. 1980; 34:490–496. [PubMed: 6246277]

Skup D, Zarbl H, Millward S. REGULATION OF TRANSLATION IN L-CELLS INFECTED WITH REOVIRUS. Journal of Molecular Biology. 1981; 151:35–55. [PubMed: 7328654]

Smith JA, Schmechel SC, Raghavan A, Abelson M, Reilly C, Katze MG, Kaufman RJ, Bohjanen PR, Schiff LA. Reovirus induces and benefits from an integrated cellular stress response. Journal of virology. 2006; 80:2019–2033. [PubMed: 16439558]

Sonenberg N, Guertin D, Cleveland D, Trachsel H. Probing the structure of the eucaryotic 5′ cap structure by using a monoclonal antibody directed against cap-binding proteins. Cell. 1981; 27:563–572. [PubMed: 6101207]

Tacken MG, Thomas AA, Peeters BP, Rottier PJ, Boot HJ. VP1, the RNA- dependent RNA polymerase and genome-linked protein of infectious bursal disease virus, interacts with the carboxy-terminal domain of translational eukaryotic initiation factor 4AII. Arch Virol. 2004; 149:2245–2260. [PubMed: 15503210]

Takacs JE, Neary TB, Ingolia NT, Saini AK, Martin-Marcos P, Pelletier J, Hinnebusch AG, Lorsch LR. Identification of compounds that decrease the fidelity of start codon recognition by the eukaryotic translational machinery. RNA. 2011; 17:439–452. [PubMed: 21220547]

Treder K, Kneller EL, Allen EM, Wang Z, Browning KS, Miller WA. The 3′ cap- independent translation element of Barley yellow dwarf virus binds eIF4F via the eIF4G subunit to initiate translation. RNA. 2008; 14:134–147. [PubMed: 18025255]

Urbonavicius J, Qian Q, Durand JM, Hagervall TG, Björk GR. Improvement of reading frame maintenance is a common function for several tRNA modifications. EMBO J. 2001; 20:4863–4873. [PubMed: 11532950]

Vende P, Piron M, Castagne N, Poncet D. Efficient translation of rotavirus mRNA requires simultaneous interaction of NSP3 with the eukaryotic translation initiation factor eIF4G and the mRNA 3′ end. J Virol. 2000; 74:7064–7071. [PubMed: 10888646]

Vera-Otarola J, Soto-Rifo R, Ricci EP, Ohlmann T, Darlix JL, López-Lastra M. The 3′ untranslated region of the Andes hantavirus small mRNA functionally replaces the poly(A) tail and stimulates cap-dependent translation initiation from the viral mRNA. J Virol. 2010; 84:10420–10424. [PubMed: 20660206]

Wakiyama M, Futami T, Miura K. Poly(A) dependent translation in rabbit reticulocyte lysate. Biochimie. 1997; 79:781–785. [PubMed: 9523021]

Walsh D, Arias C, Perez C, Halladin D, Escandon M, Ueda T, Watanabe-Fukunaga R, Fukunaga R, Mohr I. Eukaryotic translation initiation factor 4F architectural alterations accompany translation initiation factor redistribution in poxvirus-infected cells. Mol Cell Biol. 2008; 28:2648–2658. [PubMed: 18250159]

Wang Z, Treder K, Miller WA. Structure of a viral cap-independent translation element that functions via high affinity binding to the eIF4E subunit of eIF4F. J Biol Chem. 2009; 284:14189–14202. [PubMed: 19276085]

Wu B, White KA. A primary determinant of cap-independent translation is located in the 3′-proximal region of the tomato bushy stunt virus genome. J Virol. 1999; 73:8982–8988. [PubMed: 10516004]

Zarbl H, Skup D, Millward S. Reovirus Progeny Subviral Particles Synthesize Uncapped Messenger-Rna. Journal of virology. 1980; 34:497–505. [PubMed: 7373718]

- The UTRs of MRV M3 mRNA do not possess cis-acting sequences/structures necessary for translation.
- MRV M3 mRNA initiates translation using a 5′ end-dependent, scanning mechanism.
- The MRV M3 mRNA does not require the 3′ UTR or 5′-3′ UTRs interaction for translation initiation.
- The MRV M3 mRNA follows the translation initiation pattern in Kozak's context.
- The 3′ UTR of MRV M3 transcript does not affect the MRV viability or infection.

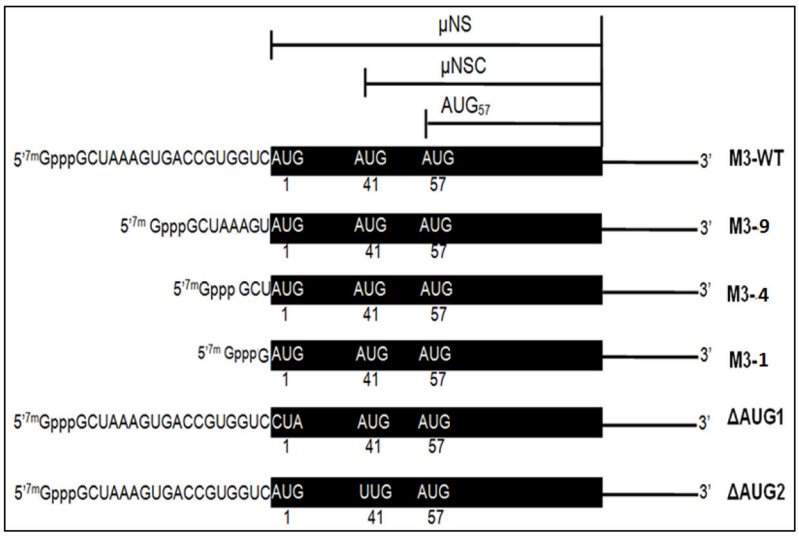

Figure 1. Schematic representation of the bicistronic MRV M3 mRNA

The MRV M3 mRNA encodes two carboxy-coterminal proteins, μNS and μNSC. Translation of μNS initiates at the 5′ proximal AUG, whereas translation of μNSC initiates at the second AUG codon (amino acid position 41). A third in frame translation product, herein denoted AUG_{57}, putatively initiates from the third AUG codon (amino acid position 57). WT M3 mRNAs possess 5′ UTRs that are 18 nucleotides in length. M3-9 mRNAs possess 5′ UTRs 8 nts in length (nts 9–18 were deleted), M3-4 mRNAs possess 5′ UTRs 3 nts in length (nts 4–18 were deleted), and M3-1 mRNAs possess 5′ UTRs comprising a single G residue. ΔAUG1 encodes a full-length M3 mRNA in which the 5′ proximal AUG codon was mutated to CUA, and ΔAUG2 encodes a full-length M3 mRNA in which the second AUG codon was mutated to UUG.

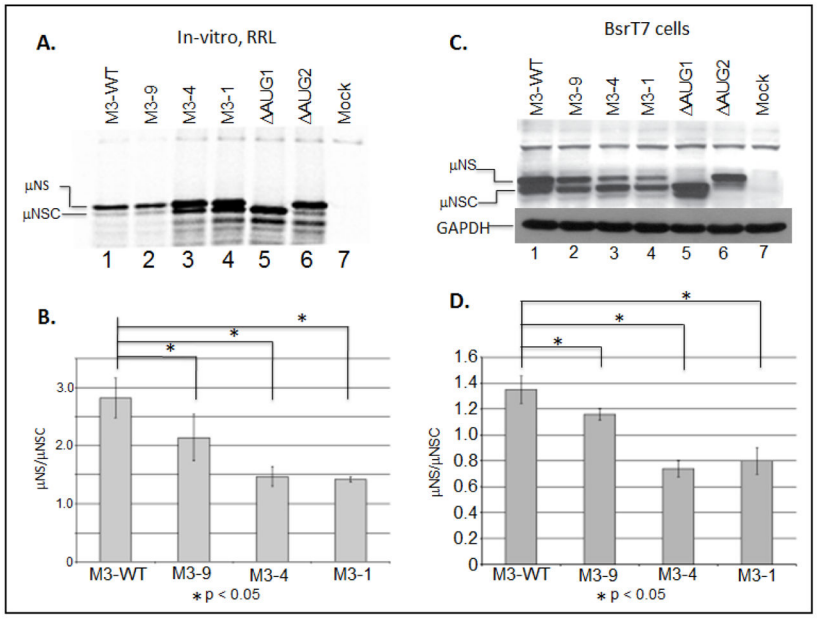

Figure 2. The MRV M3 mRNA 5′ UTR is not necessary for translation initiation but does influence start site selection

A) In-vitro RRL translation reactions were programmed with 2 μg of M3-WT, M3-9, M3-4, or M3-1 mRNAs. Reactions were incubated with [^{35}S]methionine at 30°C for 90 minutes. Reactions were stopped by addition of 2X Laemmli sample buffer and labeled proteins were separated by 8% SDS-PAGE. Labeled proteins were visualized by phosphorimaging. B) Radiolabeled μNS and μNSC proteins were quantified using ImageQuant 7.0 software. μNS/μNSC ratios were determined for each mRNA construct. μNS/μNSC ratios are presented as the arithmetic mean ± SD of three independent assays in which samples were analyzed in triplicate. Significance was determined by Student's t-test where $P<0.05$ was considered significant. C) In-vitro transcribed M3-WT and mutant construct mRNAs were transfected into BsrT7 cells. At 24h p.t. cells were lysed and μNS, μNSC and GAPDH proteins were detected by Immunoblotting. D) μNS and μNSC protein concentrations were determined by densitometry, and μNS/μNSC ratios were calculated and plotted. μNS/μNSC ratios are presented as the arithmetic mean ± SD of three independent assays with different preparations of RNA in which samples were analyzed in triplicate. Significance was determined by Student's test where $P<0.05$ was considered significant.

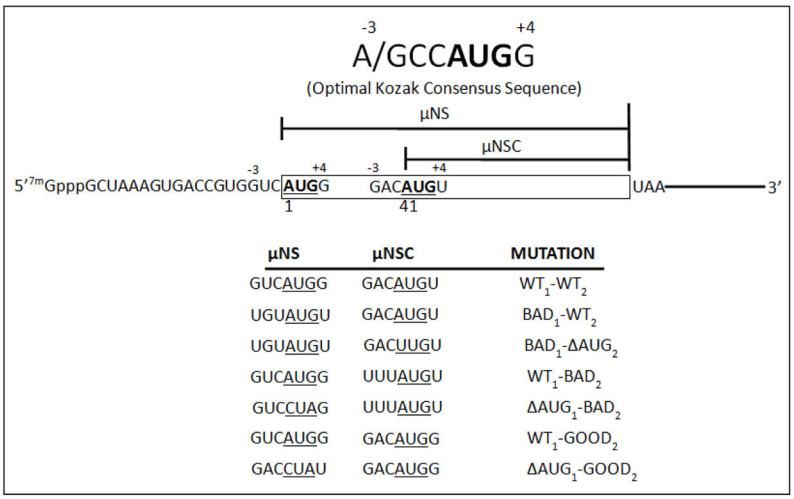

Figure 3. Schematic representation of the Kozak context of the upstream (μNS) and downstream (μNSC) initiation sites of the MRV M3 mRNA

The upstream (μNS) initiation site resides in a near optimal Kozak context; thus mutations were designed to reduce the frequency of translation initiation from this site (Bad_1). The downstream (μNSC) initiation site, however, resides in a sub-optimal context, in that a U residue occupies the critical +4 position. As such, mutations were design to either improve ($Good_2$) or further impair (Bad_2) the frequency of translation initiation from this site.

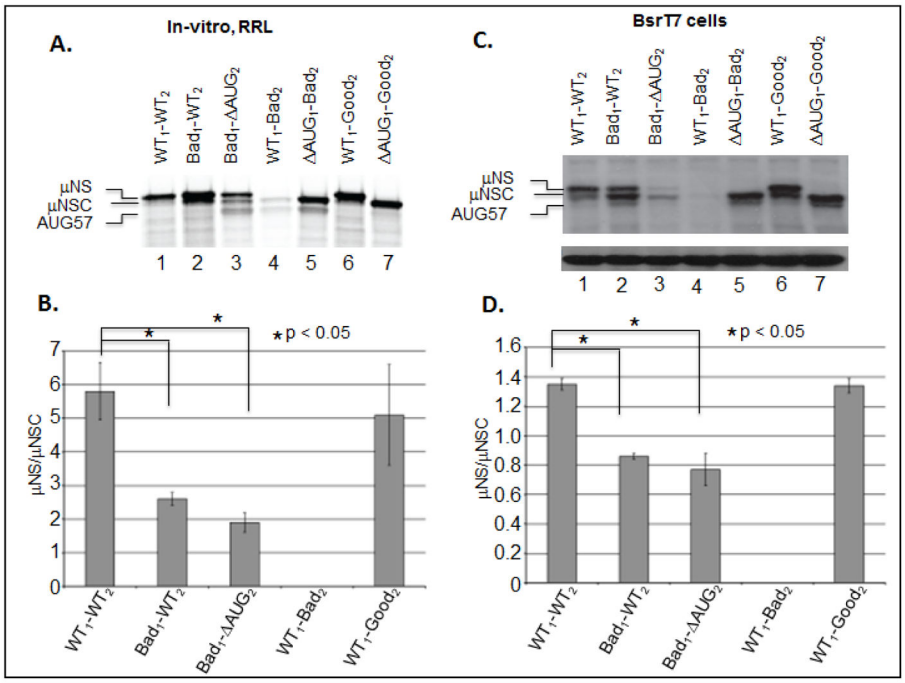

Figure 4. Altering the Kozak context of either the upstream or downstream initiation sites of the MRV M3 mRNA alters the μNS/μNSC ratio

A) In-vitro RRL translation reactions were programmed with 2 μg of WT, Kozak mutant mRNAs. Reactions were incubated with [^{35}S]methionine at 30°C for 90 minutes. Reactions were stopped by addition of 2X Laemmli sample buffer and labeled proteins were separated by 8% SDS-PAGE. Labeled proteins were visualized by phosphorimaging. B) Radiolabeled μNS and μNSC proteins, visualized by phosphorimaging, were quantified using ImageQuant 7.0 software. μNS/μNSC rations were determined for each mRNA construct (ΔAUG1 constructs were excluded from analysis). μNS/μNSC rations are presented as the arithmetic mean ± SD of three independent assays in which samples were analyzed in triplicate. Significance was determined by Student's t-test where $P<0.05$ was considered significant. C) In-vitro transcribed WT and mutant construct mRNAs were transfected into BsrT7 cells. AT 24 h p.t. cells were lysed and μNS, μNSC and GAPDH proteins were detected Immunoblotting. D) μNS and μNSC protein concentrations were determined by densitometry, and μNS/μNSC ratios were calculated and plotted. μNS/μNSC rations are presented as the arithmetic mean ± SD of three independent assays with different preparations of RNA in which samples were analyzed in triplicate. Significance was determined by Student's t-test where $P<0.05$ was considered significant.

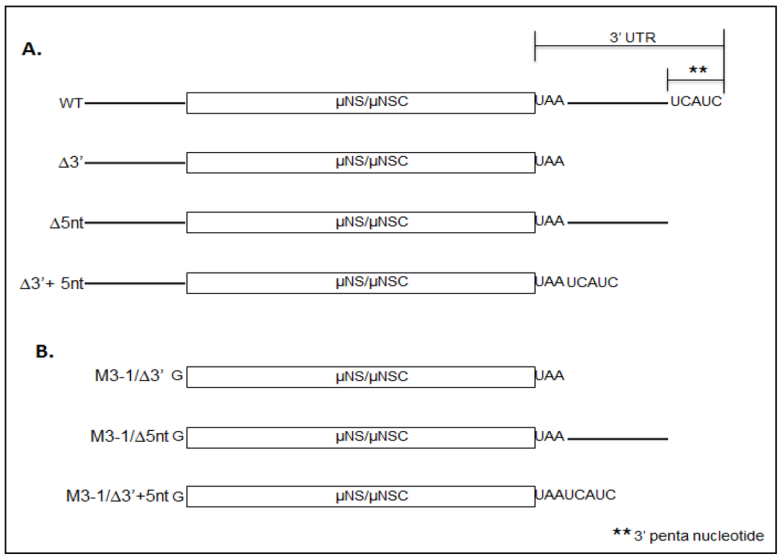

Figure 5. Schematic diagram of MRV M3 mRNA 3 UTR mutants

A) WT MRV M3 mRNA 3′ UTR comprises a 5 base conserved pentanucleotide sequence (5′-UCAUC$_{OH}$-3′) and a 55 base intervening sequence (solid line). Mutations were designed to remove the entire 3′ UTR (M3-Δ3′), the 3′ conserved pentanucleotide (M3-Δ5nt), or the 55 base intervening sequence (M3-Δ3′+5nt). B) To investigate the role of 5′-3′ interactions necessary for MRV M3 mRNA translation we engineered the Δ3′, Δ5nt and Δ3′+5nt mutations into our M3-1 mRNA construct.

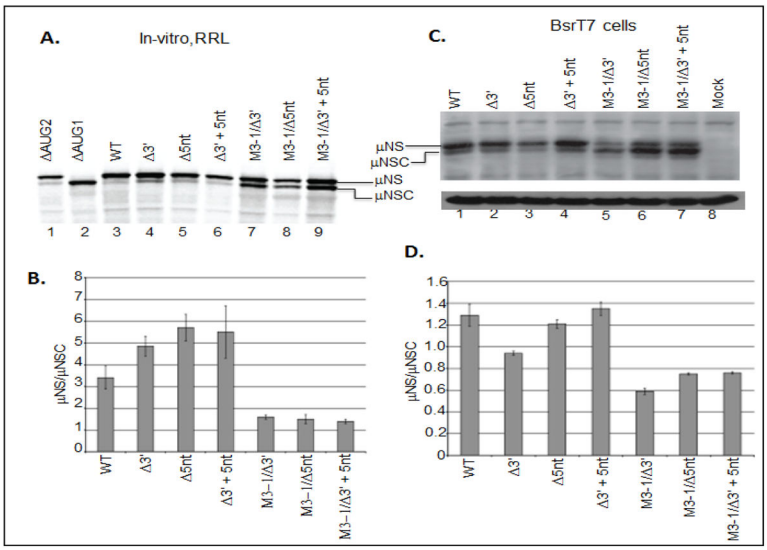

Figure 6. The MRV M3 mRNA 3′ UTR is not necessary for efficient translation

A) In-vitro RRL translation reactions were programmed with 2 μg of M3-WT or 3′ mutant mRNAs. Reactions were incubated with [^{35}S]methionine at 30°C for 90 minutes. Reactions were stopped by addition of 2X Laemmli sample buffer and labeled proteins were separated by 8% SDS-PAGE. Labeled proteins were visualized by phosphorimaging. B) Radiolabeled μNS and μNSC proteins, visualized phosphorimaging, were quantified using ImageQuant 7.0 software. μNS/μNSC ratios were determined for each mRNA construct. μNS/μNSC ratios are presented as the arithmetic mean ± SD of three independent assays in which samples were analyzed in triplicate. Significance was determined by student's t-test where $P<0.05$ was considered significant. C) In-vitro transcribed M3-WT and mutant construct mRNAs were transfected into BsrT7 cells. AT 24h p.t. cells were lysed and μNS, μNSC and GAPDH proteins were detected by Immunoblotting. D) μNS and μNSC protein concentrations were determined by densitometry, and μNS/μNSC ratios were calculated and plotted. μNS/μNSC rations are presented as the arithmetic mean ± SD of three independent assays with different preparations of RNA in which samples were analyzed in triplicate. Significance was determined by Student's t-test where $P<0.05$ was considered significant.

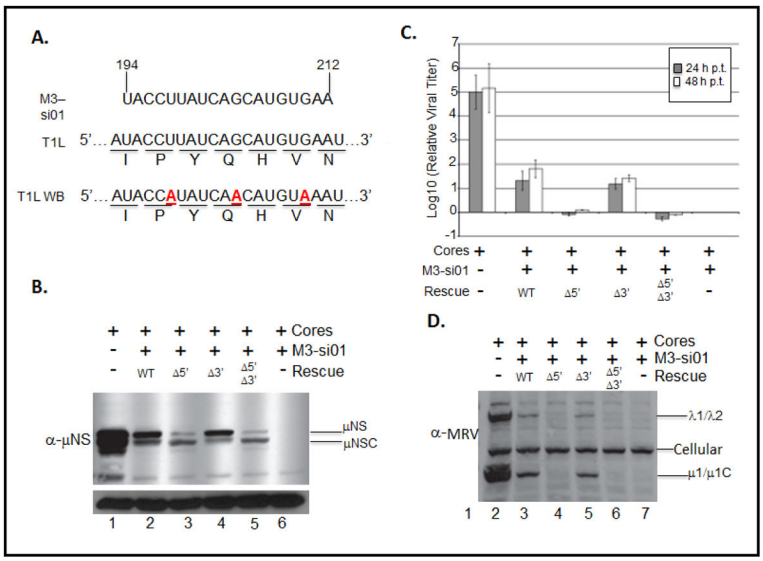

Figure 7. The MRV M3 mRNA 3′ UTR is not necessary for efficient translation initiation or start site selection in MRV T1L core transfected cells

A) M3 si-01 targets nts 194–212 of the T1L strain of MRV. The corresponding nucleotide and amino acid sequences are depicted. Mismatched bases in the wobble base rescue construct (T1L-WB) are in boldface and are underlined in the gene sequence. BsrT7 cells were transfected or mock transfected with M3 si-01. AT 6 h p.t., CsCl purified MRV T1L core particles (4×10^8 particles) were transfected with or without WT or mutant T1L-WB rescue plasmids. At 24 hrs post transfection cells were harvested and clarified lysates were analyzed by Immunoblotting to detect. B) μNS and μNSC proteins or D) MRV proteins. C) MS si-01 treated L929 cells transfected with MRV T1L core particles with or without WT or mut T1L-WB rescue RNAs were harvested at 0, 24, and 48 h p.t. by repeated freeze-thaw cycles (−80°C and 37°C), and relative viral titers were determined by conducting plaque assays on L929 mouse fibroblasts and expressed as log10 (relative viral titer).

Table 1

Forward and Reverse primers used to generate M3 (μNS or μNSC) mutants:

Mutations	Forward mutagenesis primers (5′-3′)	Reverse mutagenesis primers (5′-3′)
5′ UTR mutagenesis primers		
M3-9	CACTATAGGCTAAAGTΔATGGCTTCATTCAAGGGATTCTCCG	TGAATGAAGCCATΔACTTTAGCCTATAGTGAGTCGTATTAATTTCG
M3-4	CGACTCACTATAGGCTΔATGGCTTCATTCAAGGGATTCTCCG	CTTGAATGAAGCCATΔAGCCTATAGTGAGTCGTATTAATTTCG
M3-1	CGACTCACTATAGΔATGGCTTCATTCAAGGGATTCTCCGTC	GACGGAGAATCCCTTGAATGAAGCCATΔCTATAGTGAGTCG
ΔAUG1	AAAGTGACCGTGGTCCTAGCTTCATTCAAGGGATTCTCC GTC	CCCTTGAATGAAGCTAGGACCACGGTCACTTTAGCCTAT AG
ΔAUG2	CACTCCGTCTGTAGACTTGTCTCAATCGCGTGAATTCCTTACAAAGGC	GTAAGGAATTCACGCGATTGAGACAAGTCTACAGACGGAGTGAAGGG
Kozak's mutagenesis primers		
Bad_1	CTAAAGTGACCGTGTGTATGTCTTCATTCAAGGGATTCTCC	GGAGAATCCCTTGAATGAAGACATACACACGGTCACTTTAG
Bad_2	CACTCCGTCTGTATTTATGTCTCAATCGCGTGAATTCC	GGAATTCACGCGATTGAGACATAAATACAGACGGAGTG
$Good_2$	CACTCCGTCTGTAGACATGGCTCAATCGCGTGAATTCC	GGAATTCACGCGATTGAGCCATGTCTACAGACGGAGTG
3′ UTR mutagenesis primers		
Δ3′	GTTCCAACTGATGAGCTGTAAΔGGGTCGGCATGGCATCTCCA	GAGATGCCATGCCGACCCΔTTACAGCTCATCAGTTGGAAC
Δ5 nt	AAGCCTTCCCGACCCCTATΔGGGTCGGCATGGCATCTCCA	GAGATGCCATGCCGACCCΔATAGGGGTCGGGAAGGCTT
Δ3′ + Δ5 nt	GTTCCAACTGATGAGCTGTAATCATCΔGGGTCGGCATGGCATCTCCA	GAGATGCCATGCCGACCCΔGATGATTACAGCTCATCAGTTGGAAC
Wobble base mutagenesis primers		
pBOS36 wobble base	GGGTCTATGTCTATACCATATCAACATCATGTAAATGTTCAAAAAGTTG	CAACTTTTGGAACATTTACATGTTGATATGGTATAGACATAGACCC

"Δ" indicates deleted regions. Underline nucleotides indicate changes made in optimal context of initiation codons to favor or disfavor the translation initiation.